

**INVESTIGATING THE TEMPORAL EVOLUTION OF THE
CEREBRAL HEMODYNAMIC RESPONSE USING DIFFUSE
OPTICAL TOMOGRAPHY**

A dissertation
submitted by:

Andrew M. Siegel

In partial fulfillment of the requirements
for the degree of

Doctor of Philosophy

in

Electrical Engineering

TUFTS UNIVERSITY

May 2004

ADVISER: David A. Boas, Ph.D.

Abstract

INVESTIGATING THE TEMPORAL EVOLUTION OF THE CEREBRAL HEMODYNAMIC RESPONSE USING DIFFUSE OPTICAL TOMOGRAPHY

The primary goal of this dissertation is to provide evidence to support the hypothesis that near-infrared optical measurement of brain function relies upon similar neurovascular coupling mechanisms and measures the same hemodynamic changes as does functional magnetic resonance imaging. To test this assertion, instrumentation was constructed and methodologies were developed to replicate a sequence of rodent experiments in which an electrical stimulus to the forepaw elicited a spatially localized hemodynamic response within the somatosensory region of the cerebral cortex. The temporal evolution of this response, previously measured with functional magnetic resonance imaging, was then measured using diffuse optical tomography, and the results of both measurements are compared and discussed.

In order to perform these experiments, a number of technical issues had to be addressed. Instrumentation capable of acquiring noninvasive real-time imagery of vascular events within the cerebral cortex with minimal temporal distortion had to be designed and tested. This investigation led to the evolution of a series of optical tomographic instruments and the development of a new optical source encoding technique, Pulse TDM, which provides for advanced capabilities like individualized gain control, while significantly reducing the degree of temporal skew in the optical data.

Special surgical and anesthetic techniques which maintained normal cerebral hemodynamic activity while providing sufficient analgesia for stereotactic headgear had to be learned and mastered. To meet this need, custom surgical, biomonitors, anesthesia, and stimulus equipment was developed.

Although the temporal hemodynamic measurements themselves comprise the core of this dissertation, they represent only a small fraction of the work involved in reaching that goal. To emphasize this point, the dissertation includes chapters which discuss topics vital to biophysical experimentation, including vascular physiology, electro-optical instrument design, and anesthesia.

The ethical implications of experimentation with live subjects is a topic which is often eschewed by many researchers in the field of biophysics. Because this is an important topic, the ethical and legal responsibilities involved in animal and human experimentation are discussed in the Appendix.

Since some electronic components are common to many DOT instruments, a number of datasheets are included in the Appendix as a convenience for the more technically-minded readers. Likewise, complete schematics of the bioinstrumentation developed for these measurements is provided, in an effort to assist others in replicating this circuitry for their own research.

Acknowledgements

As an inevitable consequence of my decision to pursue my doctoral degree part-time, the majority of my efforts were spent at home or in the lab. I thus had little time to enjoy the freedoms of being a graduate student, and probably appeared to others as impatient at times (which was true, since I had to accomplish in one day the various and sundry beaurocratic tasks which others had five days to perform). As a result, I needed to rely on the assistance of my colleagues and friends, perhaps in different ways than would others. To all of you whom I may have offended or annoyed in my quest for alacrity – thank you for putting up with me. I hope that the Tootsie Rolls helped . . .

To David Boas, Mark Cronin-Golomb, Ron Goldner, and Toi Vo, my most sincere thanks for your participation in my dissertation defense committee, and your willingness to attempt to assimilate the contents of a thesis nearly 450 pages in length.

I would also like to specifically thank the following people and organizations for their various contributions to my doctoral efforts:

David Boas, for allowing me the freedom to pursue my doctoral research part-time, for giving me the opportunity to pursue my work in my own way, without interference or judgement. For introducing me to a larger world of research and collaboration which I never knew existed, for introducing me to luminaries such as Britton Chance, and for allowing me to share in some of his life experiences.

Joseph Culver, for performing the image reconstructions on all of the temporal hemodynamic response measurements shown in this dissertation. Someday I will hear you play . . .

Ronald Goldner, for giving me the opportunity to work in his lab as an undergraduate almost 20 years ago, and for helping me to feel like a member of his team.

Paul Kelley, for appreciating the value of my technical skills in the development of EOTC laboratory experiments, for helping me find a position at Lincoln Laboratory, for permitting me to pursue my Ph.D. part-time, and for assisting me with some of life's other problems along the way.

Naila Jirmanus, for allowing me to develop EOTC laboratory experiments in my own way.

Gary Strangman, for spending many days (and nights) with me on our neverending search for whisker-induced fast signals in rat barrel cortex. Although it never worked, it was quite a challenge trying to get there.

John Marota, for sparking my interest in anesthesia and for being an invaluable resource of both anesthetic and surgical knowledge which I have relied upon on numerous occasions.

Christopher Moore, for teaching me the fine art of skull thinning, whisker tweaking, and many other valuable skills.

Beth Hillman, for teaching me the ins and outs of μ Soft Word when I needed it most, for encouraging me to write a larger and better thesis, and for inspiring me with her inventive ideas and her creative spirit. My dissertation may even exceed yours in length, but it can never match your style.

Edward Smolinsky, both for his help in constructing the DOT imager we now call NIRS-3, and for his willingness to offer me the use of any equipment he had, at any time, and for being a good friend.

Maria Angela Franceschini, for having dancing kitties on her homepage, for wanting to do things herself, for helping me to smile when I needed it the most, and for having a daughter who finally likes me.

Ellen Young, who patiently allowed me to regale her with my tales of experiments gone awry, for volunteering as the model for our latest line of headgear, for donating various and sundry parts which were later crafted into surgical implements, and for being a good friend when I needed one.

The organizers and vendors at the MIT Flea Market, without which most of my experimental hardware (and that of others as well) would not have been built. Special thanks to Scott Heino of Falcon medical for offering me the wounded but repairable Datex Capnomac, which allowed me to perform real-time capnometry and greatly improved the quality of my measurements.

Igor, for shamelessly volunteering to model for many of the rodent images used in this thesis. Although I cannot thank you in words, I can surely do so with Milk Bones.

Many others, not mentioned above, have also assisted me in numerous ways, and their assistance was invaluable – for this I thank you all.

We gratefully acknowledge financial support from the National Institutes of Health 1R29NS37053-01 and from the Center for Innovative Minimally Invasive Therapies (CIMIT).

Table of Contents

1: Introduction	1
2: Creating three-dimensional images with diffuse light	9
2.1 Ballistic imaging modalities.....	9
2.1.1 Advantages of ballistic imaging modalities.....	13
2.1.2 Problems with ballistic imaging modalities.....	13
2.2 Diffuse imaging in three dimensions: DOT.....	14
2.2.1 DOT measurement techniques.....	18
2.3 Optical scattering and absorption.....	21
2.3.1 Forms of optical scattering.....	22
2.3.2 Quantifying optical absorption.....	22
2.3.3 Scattering-absorption interaction.....	24
2.3.4 The three categories of light propagation.....	26
2.3.5 Partial-volume effects.....	27
2.4 Modeling light propagation in diffuse media.....	28
2.4.1 Intuitive optical transport models.....	29
2.4.2 Single particle scattering models.....	29
2.4.3 Multiple particle scattering models.....	31
2.5 Sources of optical absorption in tissue.....	35
2.5.1 Static absorbers.....	35
2.5.2 Dynamic absorbers.....	37
2.6 Sources of optical scattering in tissue.....	40
2.6.1 Static scatterers.....	40
2.6.2 Dynamic scatterers.....	41
2.7 Modeling the medium: The Forward Problem.....	41
2.7.1 Direct approaches.....	42
2.7.2 Numerical methods.....	42
2.8 3-D Image reconstruction: The Inverse Problem.....	43
2.8.1 Regularization.....	43
3: The physiology of hemodynamics: Metabolism and circulation	47
3.1 Basic mammalian metabolic physiology.....	47
3.2 Blood rheology and vascular hydrodynamics.....	50
3.2.1 Microvascular structure.....	52
3.2.2 Gas transport and diffusion.....	53
3.3 Global hemodynamics: Regulating blood pressure.....	55
3.4 Local hemodynamics: Regulating local blood flow.....	56
3.4.1 Vascular tone and the local control of blood flow.....	57
3.4.2 Neural and chemical mediation of vascular function.....	59
3.4.3 Humoral control of the vascular system.....	59
3.4.4 Neural, metabolic, and chemo-vascular interactions.....	62
3.5 Biogenic interference.....	65
3.6 The Effect of Wavelength and Optode Spacing on Image Contrast.....	70
4: The design and evolution of CW DOT instrumentation	79

4.1	Spectral, temporal, and flux ranges for DOT.....	79
4.2	Sources and detectors for DOT and NIRS.....	80
4.2.1	Optical Sources.....	80
4.2.2	Optical Detectors.....	87
4.3	Encoding Techniques.....	88
4.3.1	Source Encoding.....	88
4.3.2	Dynamic range and signal span.....	89
4.3.3	Theoretical performance limits.....	90
4.3.4	Technical issues.....	90
4.3.5	Using Individualized Gain Control to improve performance.....	93
4.4	Developing the DOT instruments.....	105
4.4.1	The Prototype DOT Imager: CW1.....	105
4.5	The “Animal” Instrument series and their progeny.....	114
4.5.1	Animal I.....	114
4.5.2	The Optical Fetal Monitor.....	115
4.5.3	Animal II.....	119
4.5.4	The NIRS3 four-wavelength system.....	119
4.5.5	Animal III.....	138
4.5.6	Gertrude.....	140
4.6	The frequency-encoded DOT imager: CW4.....	141
5:	Preparing an in-vivo experiment.....	147
5.1	Anesthesia.....	147
5.1.1	Background.....	147
5.1.2	Hardware design and development.....	158
5.1.3	Anesthesia delivery systems.....	164
5.1.4	Common anesthetic terms and definitions.....	172
5.1.5	Important gas transport laws.....	179
5.2	Biomonitoring and life support.....	180
5.2.1	Biomonitoring.....	180
5.2.2	Design and development of the biomonitor unit.....	181
5.3	Stimulation.....	188
6:	In-vivo experiments.....	191
6.1	CW DOT Measurements of Rodent Brain Function.....	191
6.2	Temporal comparison of DOT and fMRI in rodent somatosensory cortex.....	194
6.2.1	Motivation.....	320
6.2.2	Background.....	195
6.2.3	Materials and Methods.....	195
6.2.4	Results.....	198
6.2.5	Discussion.....	201
6.2.6	Conclusions.....	204
7:	General Conclusions.....	205
7.1	Hardware Section.....	205
7.2	Experimental Section.....	208

8: Appendices	212
8.1 Ethical and legal responsibilities with live subjects.....	212
8.1.1 Human Subjects.....	212
8.1.2 Animal Experimentation.....	217
8.1.3 Certification and regulatory organizations.....	221
8.1.4 My viewpoint.....	221
8.2 Datasheets useful to DOT hardware designers.....	224
8.3 Alternate designs for the anesthetic vaporizer.....	248
8.4 Alternate anesthetic concentration monitor designs.....	250
9: References	254
9.1 Endnotes.....	254
9.2 Bibliography.....	261

List of Tables

Table 1.1. Acoustic properties of various tissues within the human body.....	11
Table 3.1. The major cellular structures and fluids responsible for light scattering.....	40
Table 3.2. Metabolic properties of the typical human brain.....	48
Table 4.1. The temporal ranges of most biogenic signals of interest to DOT.....	80
Table 4.2. The effect of optode spacing on the optical attenuation range.....	89
Table 4.3. The interchannel crosstalk vs. channel number and gain value.....	99
Table 4.4. The dynamic range vs. gain span.....	99
Table 4.5. The optical-to-electrical linearity vs. gain state.....	100
Table 4.6. Our performance goals for the prototype DOT imager.....	109
Table 4.7. Results of the measurements performed on the prototype DOT imager.....	112
Table 4.8. A summary of the measured performance of the CW4 instrument.....	142
Table 4.9. A Monte-Carlo calculation which quantified the light reaching the fetus.....	118
Table 4.10. The laser diode control register settings.....	121
Table 4.11. Variable-gain preamplifier control register settings.....	122

List of Figures

Figure 1.1.	The apparent origin of light exiting a diffuse medium.....	2
Figure 2.1.	Weight distributions for C-T (left) and DOT in transmission-mode (right)	10
Figure 2.2.	The probability density function (PDF) for light	16
Figure 2.3.	Production of volume and oxygenation imagery from raw measurements.....	18
Figure 2.4.	With a CW instrument, light is modulated at an audio frequency	19
Figure 2.5.	RF-modulated light is attenuated and delayed by diffusive transport.....	20
Figure 2.6.	Sub-nanosecond laser pulses in tissue are attenuated and broadened	20
Figure 2.7.	The apparent origin of light exiting a diffuse medium.....	25
Figure 2.8.	Angular scattering models for a single spherical particle	31
Figure 2.9.	A plot of effective multiple scattering efficiency.....	33
Figure 2.10.	Irradiance vs. depth in post-mortem neonatal brain tissue.....	34
Figure 2.11.	The molar extinction coefficient of common tissue chromophores	37
Figure 2.12.	The absorption coefficient of hemoglobin, deoxyhemoglobin, and water.....	38
Figure 2.13.	Spectral absorption properties of blood vs. oxygen saturation	39
Figure 2.14.	Extinction coefficients of various forms of hemoglobin vs. wavelength.....	40
Figure 2.15.	The L-curve for a TCG reconstruction at a signal-to-noise ratio of 20 dB	46
Figure 3.1.	Relationship between pressure, flow, velocity, and cross-sectional area.....	50
Figure 3.2.	The effect of hematocrit on blood viscosity	51
Figure 3.3.	Tissue composition of the macro- and microvasculature	53
Figure 3.4.	Hemoglobin oxygen saturation curves	54
Figure 3.5.	Carbon dioxide transport in the blood.....	54
Figure 3.6.	Mechanisms responsible for systemic blood pressure regulation	56
Figure 3.7.	The vasodilatory temporal response to neuronal activation.....	57
Figure 3.8.	A typical static arterial pressure-volume curve	58
Figure 3.9.	The effects of various agonists on vascular smooth muscle tone.....	61
Figure 3.10.	Mechanisms of endothelium-dependent relaxation of vascular muscle.....	61
Figure 3.11.	Synthesis of endothelin-1 (ET-1) within the endothelium	61
Figure 3.12.	Local blood flow (CBF) exceeds (CMRO ₂) in the brain.....	62
Figure 3.13.	How cardiac and pulmonary activity modulate diffuse optical signals.....	66
Figure 3.14.	Cardiac and pulmonary signal modulation in the frequency domain.....	67
Figure 3.15.	The pressure step response from a Windkessel vascular model	68
Figure 3.16.	A diffuse optical measurement of breast tissue under compression	69
Figure 3.17.	Linear approximation to a diffuse imaging scenario.....	73
Figure 3.18.	A plot of μ_{eff} vs. the exponent value (CSTIM aACT cACT LACT).....	77
Figure 4.1.	Vertical and horizontal confinement mechanisms in laser diodes	82
Figure 4.2.	The spectral properties of multimode and singlemode laser diodes	83
Figure 4.3.	Drawing of a machined laser diode mounting fixture	84
Figure 4.4.	Properties of a typical multimode gain-guided laser diode.....	85
Figure 4.5.	The electro-optical properties of a typical IR LED.....	85
Figure 4.6.	Analog and a digital pulse drive circuits for laser diodes and LEDs	86
Figure 4.7.	Spectral characteristics of silicon and photoemissive detectors.....	88
Figure 4.8.	Block diagrams of three DOT encoding schemes discussed in the text.....	91

Figure 4.9.	The same three DOT systems equipped with individualized gain control.....	95
Figure 4.10.	The time-encoded IGC Evaluation System.....	97
Figure 4.11.	A timing diagram for the IGC Evaluation System.....	98
Figure 4.12.	The optode assembly used to perform the Valsalva measurements.....	101
Figure 4.13.	The optical hemodynamic response to Valsalva maneuvers.....	102
Figure 4.14.	A photo showing CW1 in operation.....	111
Figure 4.15.	A block diagram of the CW1 prototype DOT imager.....	111
Figure 4.16.	Schematic of a single detector phase diversity prototype system.....	114
Figure 4.17.	Pulsatile and respiratory changes modulate the reflected optical signal.....	115
Figure 4.18.	A diagram of the Optical Fetal Monitor.....	117
Figure 4.19.	A schematic diagram of the more advanced two-color version.....	118
Figure 4.20.	A simplified block diagram depicting the Pulse-TDM concept.....	123
Figure 4.21.	A timing diagram for the NIRS-3 system.....	124
Figure 4.22.	A block diagram of NIRS-3.....	125
Figure 4.23.	An image showing Gertrude in use.....	141
Figure 5.1.	The effects of various anesthetic agents on CBF and CMRO ₂	154
Figure 5.2.	Calibration curves for the anesthetic concentration monitor.....	164
Figure 5.3.	Front and side views of Sleeper I.....	166
Figure 5.4.	A block diagram of Sleeper I.....	166
Figure 5.5.	Plot of a typical motor speed-voltage curve.....	168
Figure 5.6.	A front view of Sleeper II.....	170
Figure 5.7.	A side view of Sleeper II, showing the anesthetic vaporizer.....	171
Figure 5.8.	A top view of Sleeper II, showing the major components.....	171
Figure 5.9.	A simplified block diagram of Sleeper II.....	172
Figure 5.10.	A front panel view of the biomonitor unit.....	184
Figure 5.11.	The biomonitor probe assembly.....	184
Figure 5.12.	A top view of the biomonitor circuitry.....	185
Figure 5.13.	Schematic drawings of ECG and body temperature monitor circuits.....	186
Figure 5.14.	Schematics of the arterial pressure sensor and respiration monitor.....	187
Figure 5.15.	This Datex Capnomac anesthesia monitor.....	188
Figure 5.16.	A DOT experiment in progress.....	188
Figure 5.17.	A schematic of the stimulus isolator circuit.....	190
Figure 6.1.	Spatial and temporal responses to electrical forepaw stimulation.....	192
Figure 6.2.	DOT images of rat brain function at the peak response.....	194
Figure 6.3.	A sketch of the transcutaneous cortical optode assembly.....	197
Figure 6.4.	Spatially resolved DOT images from a single rat.....	199
Figure 6.5.	DOT time courses at 3Hz stimulation for both 6 and 30 seconds.....	199
Figure 6.6.	Temporal evolution of CBV and hemoglobin concentration.....	200
Figure 6.7.	[HbO ₂] signal and FWHM vs. stimulus frequency, current, and duration.....	201

List of Abbreviations

ABG	Arterial Blood Gas (measurement)
AC	Alternating Current
ADC, A/D	Analog-to-Digital Converter
ADP	Adenosine Diphosphate
AM	Amplitude Modulation.
ANS	Autonomic Nervous System
APD	Avalanche Photodiode
AR	Antireflection (optical coating)
ART	Algebraic Reconstruction Technique
ATP	Adenosine Triphosphate
B/G	Blood/Gas partition coefficient
BNC	Bayonet Nut Connector (a standard coaxial connector)
BOLD	Blood Oxygen Level Dependent
BP	Blood Pressure
BW	Bandwidth
CBF	Cerebral Blood Flow
CBV	Cerebral Blood Volume
cc, ml	Cubic Centimeter, Milliliter (interchangeable)
CGA	The Compressed Gas Association (standardizes gas valve fittings)
cGMP	Cyclic Guanosine Monophosphate
CMOS	Complementary Metal Oxide Semiconductor
CMR_{glu}	Cerebral Metabolic Rate of glucose consumption
CMRO₂	Cerebral Metabolic Rate of Oxygen consumption
CMRR	Common-Mode Rejection Ratio
CNS	Central Nervous System
CO₂	Carbon Dioxide
cP	CentiPoise, 0.01P (a measure of viscosity)
CPAP	Constant Positive Airway Pressure
CPV	Cerebral Plasma Volume
CSF	Cerebrospinal Fluid
C-T	Computed (X-ray) Tomography
CW	Continuous Wave
CW1, CW4	Internal designations for our continuous wave DOT instruments
dB	Decibel, = 0.1 Bel
DC	Direct Current
dl	Deciliter, 100ml

DN	Digital Number (a single digital count, 1 LSB)
DNA	Deoxyribonucleic Acid
DNR	Dynamic Range
DOT	Diffuse Optical Tomography
ECG	Electrocardiogram
EDRF	Endothelium-Derived Relaxing Factor
EEG	Electroencephalogram
EMI	Electromagnetic Interference
EPI	Echo-Planar Imaging (MRI)
etCO₂	End Tidal CO ₂ (concentration)
eV	Electron-Volt
FBR	The Foundation for Biomedical Research
FDA	The United States Food and Drug Administration
¹⁸FDG	Fluoro Deoxy Glucose, made with ¹⁸ Fluorine, a radioactive isotope
FDM	Frequency-Division Multiplexing
FFT	Fast Fourier Transform
fiO₂	Fractional inspired oxygen concentration
FM	Frequency Modulation
fMRI	Functional Magnetic Resonance Imaging
FOV, IFOV	Field Of View, Instantaneous Field Of View
FWHM	Full Width at Half-Maximum
g	The anisotropy factor, for angular scattering (unitless)
GBWP	Gain-Bandwidth Product
H₂O	Water
H₂S	Hydrogen Sulfide
Hb, HbR	Deoxyhemoglobin
HbCO, COHb	Carboxyhemoglobin
HbO₂	Oxyhemoglobin
Hbt	Total Hemoglobin
Hi	Methemoglobin, Hemoglobin
HPD	Hematoporphyrin Derivative
HR	Heart Rate
HR	High Reflectivity (optical coating)
HSD	Harlan Sprague-Dawley (rat)
Hz	Hertz, cycles/sec
IACUC	Institutional Animal Care and Use Committee
I/E	Inspiration/Expiration (ratio)
I/Q	In-phase + Quadrature (demodulation).
ICG	Indocyanine Green (dye)

IDC	Insulation Displacement Connector
IEC	The International Electrotechnical Commission (a standards organization)
IF	Intermediate Frequency (demodulation)
IGC	Individualized Gain Control
IM	Intramuscular (injection)
IP	Intraperitoneal (injection)
IRB	Internal Review Board
IV	Intravenous (injection)
kcal	Kilocalorie, = 1 Calorie
kg	Kilogram, = 1000 grams
kHz	Kilohertz, = 1000Hz
ksps	Kilosamples Per Second (ADC sampling rate)
LD	Laser Diode
LDPE	Low Density Polyethylene
LED	Light Emitting Diode
LIDAR	Light Detection And Ranging
LSB	Least Significant Bit
LSF	Least Square Fit (line)
MAC	Minimum Alveolar Concentration (anesthesia)
MAP	Mean Arterial (blood) Pressure
mg	Milligram
mg/dl	Milligrams per Deciliter
MGH	Massachusetts General Hospital
MHz	Megahertz, = 1000kHz
mHz	Millihertz, = 0.001Hz
mm	Millimeter
mmHg	Millimeters of mercury column, same as Torr
MRI	Magnetic Resonance Imaging
MUR	Maximum Unambiguous Range (radar/sonar)
MUX	Multiplexer
mW	Milliwatts
n	The index of refraction, in the near-IR spectral band
N₂O	Nitrous Oxide
NAD	Nicotinamide Adenine Dinucleotide (the reduced form of NADH)
NADH	The protonated form of Nicotinamide Adenine Dinucleotide
ND	Neutral Density (attenuating filter)
NIR	The Near-Infrared spectral band, 600nm to 900nm
NIRS	Near-Infrared Spectroscopy
NIRS3	Our internal designation for a near-infrared spectroscopic instrument

nm	Nanometer
NO	Nitric Oxide
NTC	Negative Temperature Coefficient (thermistor)
O/W	Oil/Water partition coefficient
O₂	Oxygen
OCT	Optical Coherence Tomography
OFM	The Optical Fetal Monitor (equipment)
Paw	Proximal airway pressure
PCB, PWB	Printed Circuit Board, same as Printed Wiring Board
PCMCIA	Personal Computer Memory Card International Association
pCO₂	The partial pressure of carbon dioxide
PDF	Probability Density Function
PE	Polyethylene
PEEP	Positive End Expiratory Pressure
PET	Positron Emission (transaxial) Tomography
PeTA	People for the ethical Treatment of Animals
PETN	Pentaerythritol Tetranitrate
pH	The negative log of the hydrogen ion (proton) concentration
PIN	Positive-Intrinsic-Negative (lateral doping density within a photodiode)
PM	Phase Modulation
PMMA	Poly Methyl Methacrylate (acrylic plastic used for constructing optical fibers)
PMT	Photomultiplier Tube
PNS	Peripheral Nervous System
pO₂	The partial pressure of oxygen
psi	Pounds per Square Inch. 1psi = 60mmHg
PTFE	Polytetrafluoroethane, Teflon
Pulse-TDM	Pulse-Modulated Time-Division Multiplexing
PVC	Polyvinyl Chloride
QRS	The portion of the ECG waveform generated by ventricular depolarization
RBCs	Red Blood Cells, erythrocytes
RC	Resistor-Capacitor (filter)
RF	Radio Frequency
RFI	Radio Frequency Interference
RGD	Rayleigh-Gans-Debye (scattering)
RTV	Room Temperature Vulcanizing (silicone)
saO₂	Arterial oxygen saturation
SC	Subcutaneous (injection)
SCR	Silicon Controlled Rectifier (a silicon reverse-blocking triode thyristor)
SCUBA	Self-Contained Underwater Breathing Apparatus

S-D	Source-Detector (with regard to optode placement)
SHb	Sulfhemoglobin
SIRT	Simultaneous Iterative Reconstruction Technique
SMA	Surface Mount, type A (a connector style used for both RF and fiberoptics)
SNR	Signal to Noise Ratio
spO₂	Pulse-based arterial oxygen saturation
SS-TDM	Switched-Source Time-Division Multiplexing
SVD	Saturated Vapor Dilution (vaporizer), Singular Value Decomposition (math)
T	Tesla
TCG	Truncated Conjugate Gradient
TDM	Time-Division Multiplexing
TiO₂	Amorphous Titanium (IV) dioxide, also referred to as Anatase
TPSF	Temporal Point Spread Function
TSVD	Truncated Singular Value Decomposition
u_a	The absorption coefficient, with units of 1/length
um, μm	Micron, Micrometer (same)
US	Ultrasound
u_s'	The reduced scattering coefficient, with units of 1/length
UV	Ultraviolet
VAC	Volts of Alternating Current
VDC	Volts of Direct Current
VGA	Variable Gain Amplifier
VHF	Very High Frequency (a band extending from 30MHz to 300MHz)
VIC	(Anesthetic) Vaporizer-Inside-Circuit
VOC	(Anesthetic) Vaporizer-Outside-Circuit
V-Q	Ventilation-Perfusion (matching)
W	Watts (for power measurement)
ΔX	The change in "X," with respect to a previous value
[x]	The molar concentration of "x," in units of moles/liter

1: Introduction

Diffuse Optical Tomography

Diffuse optical tomography (DOT) is a noninvasive neuroimaging technique which exploits both the spectrally varying absorption and diffuse scattering nature of near-infrared light. DOT can directly and simultaneously measure concentration changes in deoxy-hemoglobin ([Hb]), oxy-hemoglobin ([HbO₂]), and total hemoglobin ([HbT] = [Hb] + [HbO₂]) in cortical tissue with excellent temporal resolution [1].

Other neuroimaging modalities, including functional Magnetic Resonance Imaging [2, 3], Positron Emission Tomography (PET) [4], magnetoencephalography (MEG) [5-7] and electroencephalography (EEG) [6] are also capable of monitoring neural and/or metabolic activity within the brain, however DOT offers a number of important advantages over many of these well-established techniques. These advantages, along with some disadvantages, will be discussed in further detail below.

fMRI has led to significant advances in neuroimaging during the last decade. It allows near real-time observation of the hemodynamic response to neuronal activation. The blood oxygen level dependent (BOLD) fMRI signal scales approximately with absolute changes in [Hb], however questions still remain about the exact relationship between the BOLD signal and the vascular response. Likewise the coupling between neural activity and the vascular response itself is poorly understood. Since MRI and DOT are based upon different fundamental principles, cross-validation can help us to better understand both the neurophysiology behind cortical activation and the biophysics behind the measurement techniques themselves.

Others have observed qualitative correspondence between the fMRI BOLD signal and diffuse optical measures of [Hb] and [HbO₂] in humans, however to date there has been no quantitative examination of the temporal correlation between fMRI and DOT. Prior measurements have revealed much about the time course and spatial extent of cerebral blood volume and BOLD signals following median nerve stimulation in a rodent model. Since this preparation has been well characterized with fMRI, it was chosen as a convenient model to cross-validate fMRI and DOT. Therefore the primary objective of the research presented in this dissertation will be to quantitatively examine the temporal correlation between fMRI and DOT measurements of the cerebral hemodynamic response. To this end, measurements of the temporal evolution of the hemodynamic response to electrical forepaw stimulation in rat somatosensory cortex with fMRI and DOT will be compared and discussed.

Spatial and temporal resolution of current neuroimaging techniques

The temporal and spatial performance of four neuroimaging techniques is depicted in Figure 1.1 [8]. MEG provides excellent temporal resolution but only modest spatial resolution [7]. fMRI offers better spatial resolution than DOT, however decreasing MRI voxel size significantly reduces the contrast-to-noise ratio of the measurements. This necessitates the averaging of multiple trials to provide useable images. DOT can provide excellent temporal response, however its spatial resolution is limited by the diffuse nature of scattered light, which must travel through the scalp and skull twice before being detected. Since PET measurements entail the injection of a short-lived radionuclide and the monitoring of its subsequent nuclear decay, its temporal response is on the order of many minutes, which is inadequate for capturing cerebral metabolic activity in real-time.

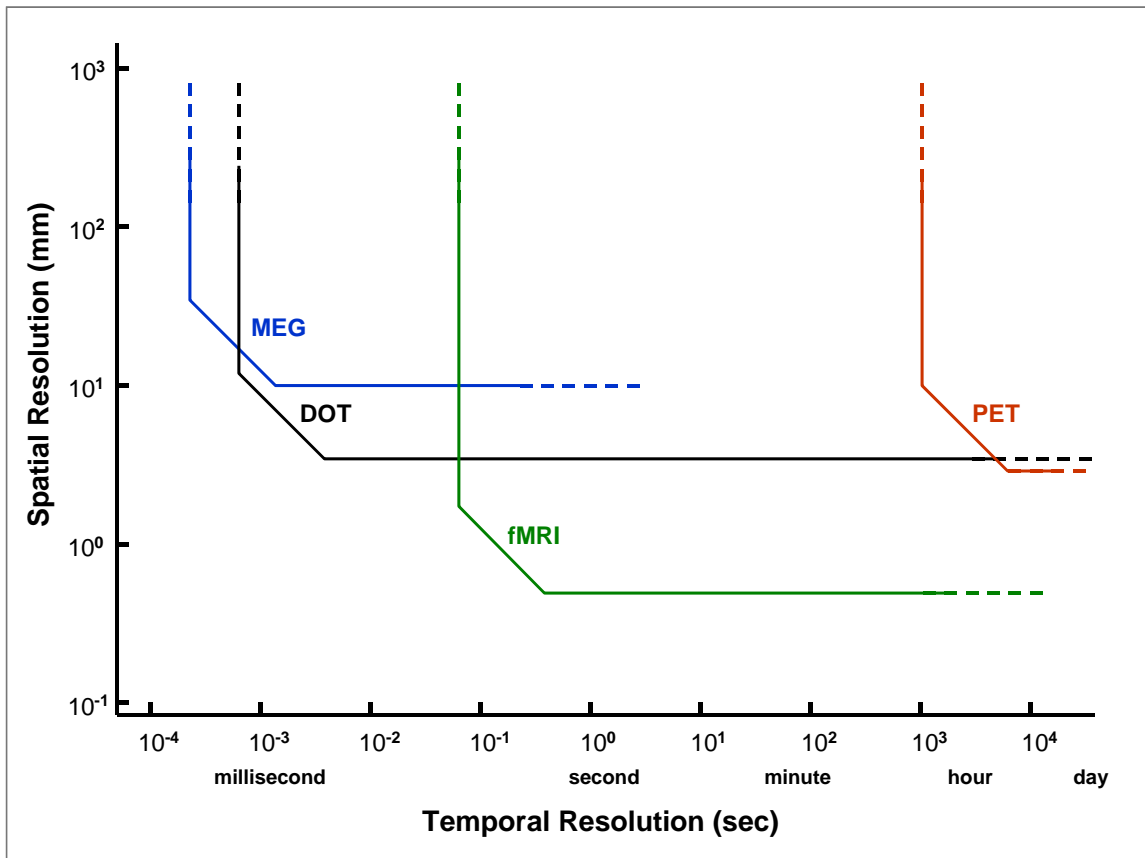


Figure 1.1. A notional diagram comparing the spatial and temporal performance of four minimally invasive neuroimaging techniques. The diagonal “chamfers” represent the improvement in spatial resolution with increased measurement time, a feature of all four modalities. MEG can provide excellent temporal resolution, but only modest spatial resolution. fMRI offers better spatial resolution than DOT, but this comes with a cost of only modest temporal response. DOT can provide excellent temporal response, perhaps rivaling MEG, however its spatial resolution is limited by the diffuse nature of scattered light in tissue [8]. PET can monitor cerebral metabolic activity with spatial resolution comparable to DOT, however each measurement requires about 10 minutes to complete, so real-time monitoring of metabolic activity is not possible [4].

Potential disadvantages of MEG and fMRI as neuroimaging tools

DOT offers a number of important advantages over both MEG and fMRI, both of which involve the use of large, heavy, and expensive equipment. Often, an entire portion of a building must be dedicated to these measurements, since elaborate magnetically shielded enclosures must be constructed to both shield the equipment from ambient magnetic fluctuations and in certain cases (high-field MRI) to protect the outside environment from the emanation of stray magnetic fields.

Both require the use of cryogenics or mechanical coolers to maintain temperatures low enough to sustain superconduction. Modern fMRI systems employ superconducting magnets to provide the large (1.5 to 7 Tesla) static magnetic field to induce proton precession and MEG systems use superconducting Josephson junctions to detect very small changes in magnetic field caused by electronic and ionic currents within the brain [7].

Both MEG and fMRI also require that the subject remain motionless to within the order of a voxel over the duration of the experiment, or else spatial resolution could be severely compromised. This makes both MRI and MEG measurements of uncooperative subjects (animals and infants, for example)

nearly impossible without pharmacologic intervention. Although anesthesia will render a subject motionless for many hours, it can also severely affect normal neural function, while making voluntary response measurements nearly impossible.

Potential advantages of DOT over MEG and fMRI for neuroimaging

DOT systems can be constructed to be physically compact, lightweight, and energy-efficient [9, 10]. Portable DOT systems can be constructed to conform to just about any environment which is compatible with human life. Since DOT can employ flexible fiberoptic light guides, a modest amount of motion can be tolerated during DOT measurements [8, 10]. Monitoring the regional cerebral blood volume and oxygenation of infants in the NICU, astronauts in orbit, or technical divers undergoing decompression – feats clearly difficult or even impossible with fMRI or MEG – are possible with DOT.

An important feature of DOT not shared by fMRI or MEG is the capability to rapidly and simultaneously measure changes in both local cerebral blood volume (CBV), deoxyhemoglobin concentration ([Hb]), and oxyhemoglobin concentration ([HbO₂]) within the brain [8, 11]. fMRI can measure changes in blood volume, but is only sensitive to absolute changes in deoxyhemoglobin, from which blood oxygenation changes must then be inferred [12]. PET can measure the cerebral metabolic rate of glucose consumption (CMR_{glu}), the cerebral metabolic rate of oxygen consumption (CMRO₂), and cerebral blood flow (CBF), however each measurement can take more than 10 minutes to complete [4, 13].

Since DOT can provide capabilities unavailable with any other neuroimaging techniques, there is significant interest in better understanding the capabilities and limitations of DOT as a neuroimaging modality.

Features of DOT

DOT is painless, noninvasive, and simple to use. It can be performed inexpensively and safely on nearly any patient at any time, in contrast to other imaging modalities like C-T and MRI. If the optode assemblies are properly designed, patients are afforded more freedom of movement during DOT imaging than with either C-T or MRI. Since DOT equipment can be portable, the DOT system can be wheeled to the patient, instead of vice-versa, thus reducing the added risk to the patient.

Spectroscopic information about the sample can be obtained in real-time. This can then be processed to yield three-dimensional maps of both blood oxygenation and CBV vs. time. With DOT, exogenous contrast agents are not required, and metabolic information can be monitored continuously, unlike with PET.

Limitations of DOT

DOT can provide only limited spatial resolution, which decreases with increasing penetration depth. This is an unavoidable consequence of the nature of diffusely scattered light: there is an inexorable increase in entropy, and hence a loss in spatial information, as the result of every scattering event which occurs inside the tissue. Although DOT cannot replace either MRI or C-T for obtaining deep tissue metabolic and structural information, it will likely serve as an adjunct to such modalities, providing details on metabolism and perfusion in human subjects not easily obtained otherwise.

Problems with performing accurate DOT include compensating for partial-volume effects and the loss in hemodynamic specificity at the sub-millimeter level, possibly due to significant contributions from surface vessels [14]. (fMRI has shown that CBF changes remain specific, even down to sub-mm functional domains [15]).

Uncertainties with fMRI and DOT as neuroimaging tools

fMRI is currently one of the preferred modalities for neuroimaging because it can provide both structural and metabolic information. Since fMRI and DOT are both believed to monitor brain function indirectly through measurements of blood flow and blood oxygenation changes within the brain, yet require vastly differing financial investments to construct and operate, it is important to explore the relative merits of DOT as a modality for neuroimaging applications. If fMRI and DOT share similar spatial, temporal, chemical, and vascular sensitivities throughout the cerebral cortex, then DOT could serve as a simple, safe, and low-cost substitute for fMRI in many neuroimaging applications.

If, on the other hand, fMRI and DOT differ in one or more of these sensitivities, then the possibility exists that, to the extent of their orthogonality, both techniques may complement each other, thus providing an augmented neuroimaging capability unavailable from each technique used independently.

However, in order to exploit the benefits of either case, the exact nature of how and what each modality measures in-vivo must be determined. Simply combining the data from a new, yet poorly understood, modality with that from another well-characterized modality would result in little, if any, additional knowledge.

fMRI appears to be uniformly sensitive to blood flow and oxygenation changes within the volume of the brain, except in the regions surrounding large blood vessels [12]. Although the mechanisms underlying the use of superparamagnetic contrast agents to monitor changes in Cerebral Blood Volume (CBV), or more correctly, Cerebral Plasma Volume (CPV) are well understood [12, 16, 17], evidence for the origin of the Blood Oxygen Level Dependent (BOLD) signal is still not conclusive [12]. It is believed to result from the metabolic reduction of slightly diamagnetic oxyhemoglobin (HbO_2) to form weakly paramagnetic deoxyhemoglobin (Hb). The Hb then perturbs the local magnetic environment, thus generating the BOLD signal. As a result, the carrier to noise ratio of the CBV measurement is proportional to the fractional change in CBV, while the carrier to noise ratio of the BOLD signal is proportional to the absolute change in [Hb] [12].

DOT, on the other hand, shows greater sensitivity to flow and oxygenation changes in vessels closer to the cortical surface [14, 18], although the sensitivity near large vessels may actually be reduced [18]. This follows from the volume weighting function for DOT, illustrated by Figures 1.1 and 2.2, which show proportionally greater sensitivity to blood volume and oxygenation changes occurring nearer to the optodes and within the “banana.” The light transiting larger vessels may be so strongly absorbed that, despite the large modulation depth imposed by the high blood volume fraction, the amount of light actually reaching the sensing optode may fall below the detector noise floor and thus be missed [18].

Research objectives and issues to be addressed within this dissertation

This dissertation will attempt to answer some of these questions by comparing DOT and fMRI measurements of the temporal evolution of the cerebral hemodynamic response.

Many researchers have observed qualitative spatial [19-21] and temporal [22] correspondence between the fMRI BOLD signal and diffuse optical measures of deoxyhemoglobin concentration ([Hb]) and oxyhemoglobin concentration ($[\text{HbO}_2]$) in humans. However to date there has been no quantitative examination of the temporal correlation between fMRI and DOT in similar preparations. The observation that the rise in Cerebral Blood Flow (CBF) in upper cortical layers preceded the rise in lower layers [23] suggests that differences in the volume weighting functions between fMRI and DOT may be revealed through comparison of temporal measurements of the cerebral hemodynamic response by both modalities.

Previous measurements of rat somatosensory cortex have revealed much about the time course and spatial extent of CPV and BOLD signals following median nerve stimulation in a rodent model [12, 16, 17, 24-27].

Since the rodent forepaw stimulation preparation has been well characterized with fMRI, and due to its geometry, would afford a similar spatial matching in voxel size between fMRI and DOT, it was chosen as a convenient model to cross-validate fMRI and DOT. Thus the principal objective of this dissertation will be to quantitatively compare the temporal evolution of the cerebral hemodynamic response as measured with fMRI and DOT using the rodent preparation, and to use these measurements to better understand both the matching of sensitivities between fMRI and DOT and to learn more about the origin and nature of the cerebral hemodynamic response.

Researchers using other optical imaging modalities have observed an amplitude dependence of the vascular response on stimulation parameters such as the pulse frequency and stimulus duration [28]. This is likely a fruitful topic that is relatively easy to explore with our preparation, so the effects of stimulus repetition rate, duration, and magnitude will also be investigated, both to determine the robustness of this preparation and to further explore the physiology underlying the neurovascular response.

Preparing for these rodent measurements required a significant hardware development effort. New, faster DOT systems capable of recording at frame rates sufficient to capture the temporal features of the hemodynamic response were required. Anesthesia and biomonitoring instrumentation with performance superior to that available commercially was developed in order to maintain hemodynamic stability during these experiments. Hence the secondary objective of this dissertation will be to discuss the development of the diffuse optical and biomedical instrumentation specifically designed for in-vivo DOT measurements.

Chapter summary

The first five chapters of this dissertation were written to both educate the reader in preparation for the discussion of the experimental results presented in Chapter 6, and to explore the evolution of DOT instrumentation which ultimately enabled spatially resolved measurements at frame rates fast enough to examine the temporal features of the hemodynamic response. Chapter 7 summarizes the many conclusions drawn and lessons learned throughout this dissertation, and the Appendix contains supplementary information relevant to a number of topics which may also interest the reader.

Introduction

Diffuse optical tomography is based upon the diffusive transport of light in tissue, so the principles behind DOT, and the unique nature of diffuse imaging, are briefly covered in the Introduction. In order to compare DOT with other neuroimaging techniques, the principles behind other metabolic and neuroimaging modalities, including functional magnetic resonance imaging (fMRI) in particular, are also presented. The relative merits of fMRI and DOT are mentioned, with emphasis on their similarities as neuroimaging tools. Prior research citations are then used to reveal the current level of uncertainty concerning the temporal, vascular, and spatial sensitivities of both modalities, which leads to the specific questions which motivated the pursuit of this dissertation.

Chapter 2

The concept of diffuse imaging is introduced in Chapter 2, and the basic principles of CW, RF, and time-domain instrumentation are all discussed. Chapter 2 begins by introducing the reader to the basic optical principles behind optical imaging, and then discusses light propagation and scattering in turbid media. Issues such as the pathlength correction factor and scattering anisotropy are also covered. Distinctions are made between how ballistic, “snake,” and diffusely scattered light are best modeled. The relative merits and disadvantages of both ballistic and diffuse imaging are also explored.

Since the quality of DOT image reconstruction is a direct function of the accuracy with which diffusive light transport through the medium is modeled, Chapter 2 presents a number of optical transport and scattering models for light propagation through scattering media. Multiple scattering models are then discussed, and the concepts behind the basic diffusion theory are introduced. Since the DOT measurements discussed in this dissertation were all performed in living tissue, the many sources of optical absorption and scattering in biological tissues are then presented, and the important distinction between static and dynamic absorbers and scatterers is made.

DOT image reconstruction is then discussed at an overview level. The theoretical and numerical techniques involved in reconstructing images from raw optical measurements are reviewed. Both the forward and inverse problems are explained, and a number of common algorithms are discussed. The complexities introduced by the ill-posed and underdetermined nature of the matrices involved in DOT image reconstruction are explained, and the concept of regularization is then discussed.

Chapter 3

In order to draw meaningful conclusions from diffuse optical measurements of brain function, the physiology behind neurovascular coupling and the cerebral hemodynamic response must be understood, so Chapter 3 provides a comprehensive introduction to vascular and metabolic physiology, with specific emphasis on circulation and the mechanisms underlying the hemodynamic response. Since metabolic activity generates both desirable and undesirable hemodynamic changes, Chapter 3 also addresses the issue of biogenic interference and presents some of the ways in which its effects can be mitigated.

Chapter 4

Before useful DOT measurements can be made, instrumentation capable of acquiring noninvasive real-time imagery of vascular events within the cerebral cortex with minimal temporal distortion had to be designed and tested. Many of the issues involved in the design and development of DOT instrumentation are covered in Chapter 4. An investigation into better methods of source encoding led to the development of a new optical encoding technique, Pulse-TDM, which allows for advanced capabilities like individualized gain control while providing very high dynamic range and minimal temporal skew in the optical imagery.

Chapter 4 also covers the design and construction of a variety of DOT instruments, ranging in evolution from the first tomographic system we constructed to the flexible high-speed DOT system used to perform the temporal hemodynamic response measurements discussed in Chapter 6 and still in use today. The history behind their development, plus the results of in-vivo performance evaluations and laboratory measurements used to characterize some of these instruments are also included in Chapter 6.

Chapter 5

Since custom surgical, biomonitoring, anesthesia, and stimulus equipment was required in order to perform the rodent DOT measurements, the design and development of the equipment necessary for performing in-vivo measurements of brain function in rodents are all discussed in detail in Chapter 5. Although the DOT measurements themselves are noninvasive, the need for tight metabolic monitoring and control over an uncooperative subject (a rat) necessitated the use of both stereotactic restraint and invasive procedures to obtain vascular access, so both sedation and analgesia were required. Surgical and anesthetic techniques that preserved normal cerebral hemodynamic function while providing analgesia sufficient for the use of stereotactic headgear are described.

Chapter 5 begins by discussing the pharmacology, physics and physiology behind anesthesia, followed by the design, assembly and testing of a custom anesthesia/ventilator system suitable for rodents and other small animals. Since monitoring the physiologic status of the subjects is critical to

both managing anesthesia and maintaining hemodynamic stability, the topic of biomonitors is discussed, followed by the design and development of a rodent biomonitors system.

This rodent preparation employed forepaw stimulation to generate a reproducible cerebral hemodynamic response in a localized region of the somatosensory cortex, so the issues involved in delivering stable and repeatable electrical stimuli over long periods of time are addressed, followed by the design and construction of a galvanically isolated forepaw stimulator. Complete schematics of the bioinstrumentation are provided to encourage future investigators to replicate this circuitry for their own research.

Chapter 6

Once all of the DOT, anesthesia, biomonitors, and stimulus equipment has been constructed and tested, quantitative DOT measurements could then be performed and analyzed. Since much experience was gained from forepaw stimulation measurements performed on earlier DOT systems, Chapter 6 begins by presenting forepaw stimulation data collected using our original DOT instrument: CW1. This work is then followed by a detailed description of the temporal hemodynamic response measurements performed with CW4, a faster and more flexible frequency-encoded DOT system. The imagery and temporal data are presented and the mechanisms believed to be responsible for the temporal features visible in the data are discussed and compared to similar forepaw measurements collected with functional MRI. The effects of stimulus repetition rate, duration, and magnitude were examined in an effort to determine the robustness of the rodent forepaw stimulus preparation and to further understand the physiology underlying the neurovascular response.

Chapter 7

Chapter 7 summarizes the many conclusions drawn and lessons learned throughout the body of this dissertation. The hardware section covers topics related to optical source and detector selection, source encoding, anesthesia, biomonitors, and stimulation. The experimental section then presents conclusions drawn from the rodent somatosensory cortical measurements, including observations concerning the effects of variations in forepaw stimulus current and stimulation frequency.

Appendix

The Appendix includes information that is important, yet not sufficiently salient to the main topics, to be included in the body of the dissertation. The ethical implications of experimentation with live subjects are a topic that is often eschewed by many researchers in the field of biophysics. Because this is an important topic, the ethical and legal responsibilities involved in animal and human experimentation are discussed here. Datasheets for many of the optical sources, detectors, and sensors used to construct the DOT instrumentation discussed above are also included for convenience, should the reader wish to refer to these for more information.